Chemical Engineering Journal 148 (2009) 525–532

Contents lists available at ScienceDirect

Chemical Engineering Journal

journal homepage: www.elsevier.com/locate/cej

Oxidative coupling of methane (OCM) in a catalytic membrane reactor and comparison of its performance with other catalytic reactors

Subhash Bhatia*, Chua Yen Thien, Abdul Rahman Mohamed

School of Chemical Engineering, Universiti Sains Malaysia, Engineering Campus, 14300 Nibong Tebal, Penang, Malaysia

ARTICLE INFO

Article history:
Received 29 May 2008
Received in revised form
22 December 2008
Accepted 8 January 2009

Keywords:
Oxidative coupling of methane (OCM)
Catalytic membrane reactor (CMR)
Na-W-Mn/SiO_2
Mixed ionic-electronic conducting membrane (MIECM)
Packed bed membrane reactor (PBMR)

ABSTRACT

The oxidative coupling of methane (OCM) was studied in a catalytic membrane reactor (CMR), catalyst packed bed reactor (PBR) and catalyst packed bed membrane reactor (PBMR) respectively. The CMR consists of a mixed ionic-electronic conducting membrane (MIECM) $Ba_{0.5}Ce_{0.4}Gd_{0.1}Co_{0.8}Fe_{0.2}O_{3-\delta}$ (BCGCF) coating on the outer surface of ceramic tubular support using sol–gel method. The inner surface of the membrane tube was coated with 3 components (Na-W-Mn) catalyst using mixture slurry dip coating method. Prior to the OCM reaction, separation of oxygen from the mixture of nitrogen and oxygen similar to air composition was performed in the membrane reactor. In the absence of chemical reaction, the oxygen permeation flux was 0.6 $cm^3/min\,cm^2$ at 900 °C with sweep gas flow rate 100 cm^3/min. The oxygen permeation flux increased significantly during the oxidative coupling of methane reaction. 67.4% of C_{2+} selectivity and methane conversion of 51.6% with oxygen permeation flux 1.4 $cm^3/min\,cm^2$ was obtained at 850 °C with sweep gas flow rate of 100 cm^3/min. The performances of PBR and PBMR using Na-W-Mn/SiO_2 were compared with the performance of CMR. The catalytic membrane reactor performed best among three reactors with C_{2+} yield of 34.7%. The deterioration of the catalytic membrane performance after reaction was investigated by SEM and XRD analyses.

1. Introduction

In recent years, oxidative coupling of methane (OCM) studies have been focused to the application of membrane reactor; the noteworthy technology that believed to overcome the limitation of low C_{2+} yield and minimizing the economic constraints. Various types of inorganic membranes are reported in the literature. These include inert porous membrane [1–4], packed bed membrane [5,6], catalytic membrane [7,8], solid-oxide membrane [9,10] and dense membrane [11–14]. These are classified as per their characteristics in selectivity and permeability. Both of these characteristics are determined by the interaction between the membrane and the permeating molecules which resulted in the different transport mechanisms.

Coronas et al. [1] in their study of OCM used PBMR with coating the porous α-alumina membrane (pore size 10 μm at outer layer and 200 nm at inner layer) by depositing silica sol (with sodium content) inside the porous alumina structure and further impregnating with Li_2CO_3 solution, in order to improve the membrane surface area and its acidity. Catalyst Li/MgO was packed within the tubular membrane and 28% of methane conversion, C_{2+} selectivity 60–65% and C_{2+} yield 16.8–18.2% were obtained at the operating temperature 1023 K, CH_4/O_2 ratio 4 and WHSV 4000 $cm^3/g\,h$. Another work reported using porous membrane support (Pall-Exekia) was attempted to stabilize the γ-alumina membrane tube by coating lanthanum oxide, which believed to be the most effective inhibitor in preventing the sintering of the γ-alumina at high temperature more than 700 °C with the 3-component W-Mn-Na/SiO_2 catalyst packed inside the membrane tube [5].

These research studies were ineffective in terms of ethylene yield and selectivity because porous membrane was not good in controlling oxygen perm-selectivity, and the permeability of methane to the air side might occur. In addition, the reactant stream in a packed-bed membrane reactor bypassing the catalyst packed in the reaction side may occur if there is insufficient pressure drop across the membrane. Recently, some research efforts have been directed toward searching for ionic conducting perovskite-type oxide membrane [7,11] and dense fluorite-structured membrane [12,15], which could enhance the oxygen permeation flux in membrane reactor. This, in consequence, will increase the methane conversion and thus promoting higher yield of C_2 product in OCM process. The gas phase homogeneous reaction can be reduced because the oxygen first reaches the catalyst through the membrane and forms active surface-oxygen species, and further convert methane to methyl radical that favored in OCM reaction. Haag et al. [16] reported that the oxygen flux and its permeability control

* Corresponding author. Tel.: +60 4 5996409; fax: +60 4 5941013.
E-mail address: chbhatia@eng.usm.my (S. Bhatia).

1385-8947/$ – see front matter © 2009 Elsevier B.V. All rights reserved.
doi:10.1016/j.cej.2009.01.008

the methane conversion and C_{2+} selectivity during OCM reaction in a catalytic membrane reactor using dense perovskite membrane coated with Pt/MgO catalyst. Yang et al. [13] conducted the OCM reaction in both the PBCMR and CMR and they found that the C_{2+} selectivity in CMR was limited by high ion recombination rates in the $Ba_{0.5}Sr_{0.5}Co_{0.8}Fe_{0.2}O_{3-\delta}$ dense membrane. The improvement in the C_{2+} selectivity was observed after La-Sr/CaO catalyst was packed in the membrane tube.

These results show a remarkable potential of membrane reactor in OCM, though the technological gap still exists in achieving the industrial practice. The main challenge is the fabrication of ionic conducting membrane, where solid-state reaction/isostatic pressing method (easier method) was mostly used by the researchers, which is not applicable in industry. Some researcher suggested that a uniform distribution of pore size membrane (tube/disc) available in the market should be used. This membrane should be modified by coating the desired ionic conducting material and catalyst on the membrane. Sol–gel method is one of the methods for dip coating the ionic conducting material and catalyst on the membrane [17,18].

The present research is focused on the study of OCM reaction in a catalytic membrane reactor (CMR) for the production of C_{2+} (ethane plus ethylene). CMR performance was compared with the performances of the packed bed catalytic reactor (PBR) and packed bed membrane reactor (PBMR) containing Na-W-Mn/SiO_2 catalyst. The membrane was synthesized by coating a mixed ionic-electronic conducting membrane (MIECM) $Ba_{0.5}Ce_{0.4}Gd_{0.1}Co_{0.8}Fe_{0.2}O_{3-\delta}$ (BCGCF) on the outer surface of the ceramic tubular support using sol–gel technique. The MICEM has high oxygen permeability as desired for the OCM reaction. The inner surface of the membrane tube is coated with 3 components (Na-W-Mn) catalyst using mixture slurry dip coating method to convert it as catalytic membrane.

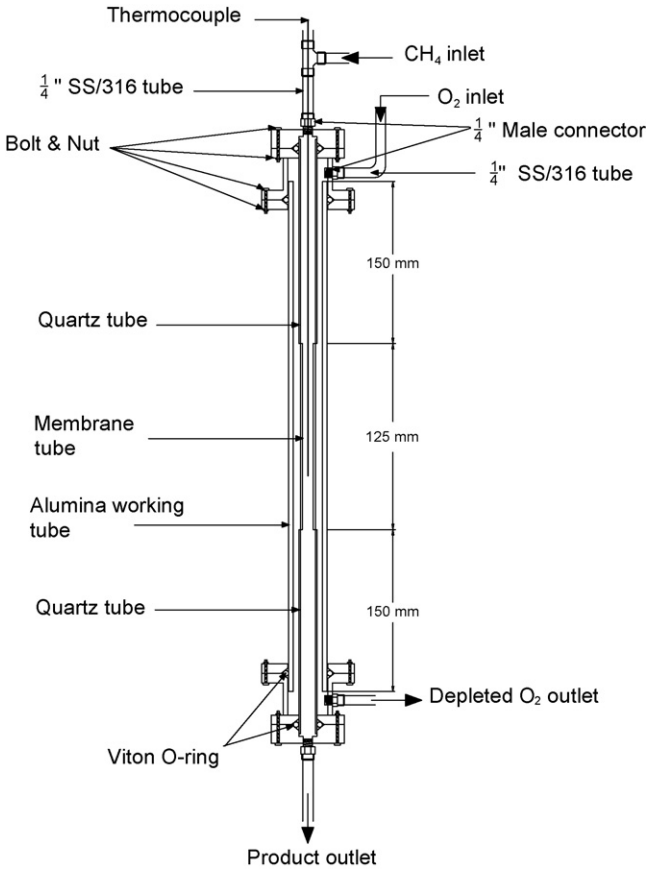

Fig. 1. Schematic drawing of catalytic membrane reactor.

2. Experimental

2.1. Synthesis of MIECM

The commercial alumina support tube (Pall-Exekia) was pretreated with 50 wt.% lanthanum nitrate aqueous solution to stabilize the gamma alumina for high temperature reaction. The outer surface of the tube was coated with a MIECM.

The MIECM with BCGCF material was prepared by combined citrate–ethylene diamine tetraacetic acid (EDTA) complex sol–gel method [19]. The lanthanum nitrate treated alumina support tube was first dip-coated into the BCGCF sol. Only the outer surface of the alumina tube was exposed to the BCGCF sol by closing both ends of the tube using a set of Teflon cap. The membrane tube was allowed to air-dry after withdrawal from the sol. The air-dried membrane tube was further dried at 100 °C for 4 h and subjected to the heat treatment at 400 °C for 4 h with heating rate of 0.2 °C/min. The dip coating and heating steps were repeated for 8–10 times. Finally, the coated membrane tube was calcined at 1000 °C for 6–10 h.

2.2. Synthesis of catalytic layer

Three components catalyst Na-W-Mn/SiO_2 was coated as a catalytic thin film on the alumina tube using mixture slurry method [20]. The membrane tube was dipped into the catalyst solution. Before the dip-coating process, the outer membrane tube was covered with poly tetra fluoro ethylene (PTFE) tape in order to prevent the coating of catalyst on the MIECM layer. The membrane tube was dried in air for an hour before overnight drying at 100 °C and calcined at 900 °C for 8 h. These steps were repeated for 3 times in order to obtain good coating of the catalytic thin film over the membrane tube.

2.3. Reactor module

The catalytic membrane reactor was designed and fabricated by considering the three major prerequisites such as, gas-tight reactor system, resistant to high temperature without any reaction with the gases and the membrane tube within the reactor could be taken out easily without breaking the membrane tube. The design of catalytic membrane reactor resembles like a shell and tube heat exchanger as shown in Fig. 1. The reactor was comprised of a highly impervious alumina working tube (length 304.8 mm × ID 25.4 mm × OD 31.4 mm) that served as the reactor casing (shell side) and the membrane tube (length 125 mm × ID 7 mm × OD 10 mm, pore size 5 nm) was connected to a quartz tube (length 150 mm × ID 10.5 mm × OD 13 mm) with sealant (Aremco, Ceramabond 569) at each end (tube side) of the membrane tube. Special care was taken during the sealant curing procedure. The sealant in slurry form was well mixed before applied to the connecting point of membrane tube and quartz tube. Then, it was kept to dry in air for 2–4 h and further to be placed in furnace for heat treatment at 550 °C for 4–6 h. After that, the sealing part was added with some thinner (Aremco, Ceramabond 569-T) and let the thinner to diffuse through the sealant and filled the pores or cracks within the seal. Viton O-ring was used to provide a gas tight seal between the alumina working tube and the quartz tube. A K-type thermocouple was placed in the reactor to indicate the temperature of the reaction zone and another one was attached to the outside wall of the reactor. As the membrane is far shorter than the length of the heating zone, the temperature gradient along the membrane was negligible. The leak test was done by purging compressed air into the reactor and it must be gas tight at the pressure of 2 bars.

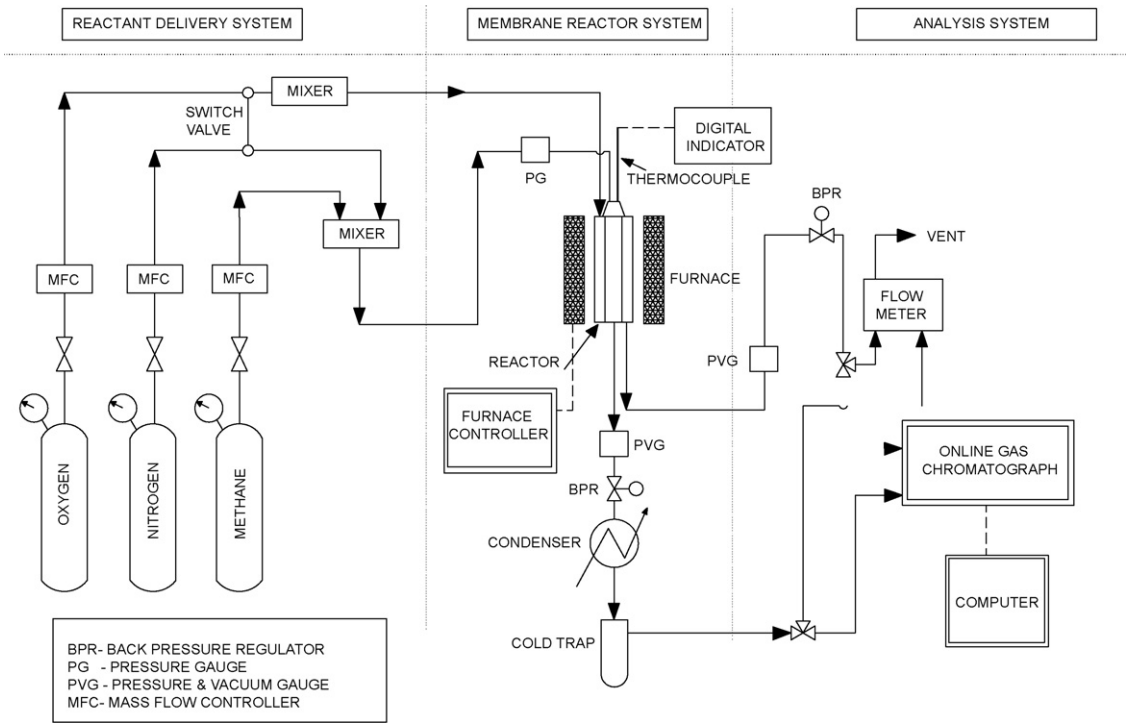

Fig. 2. Schematic diagram of experimental test rig system.

Reactant gases CH_4 (99.92%) and sweep gas helium (99.999%) were fed into the reactor from the tube side whereas mixture of oxygen (99.8%) and nitrogen (99.999%) resembling air composition were fed into the reactor from the shell side. Methane flow rate was regulated by mass flow controller (MKS, Model 246c), whereas another mass flow controllers (Brooks, 5850E) were used to regulate nitrogen and oxygen gas flow rates. A cold trap was placed at the outlet of the reactor to separate any condensed water vapor from the reaction product. Fig. 2 shows the schematic representation of the experimental set-up used in the present study.

2.4. Experimental procedure

In order to study OCM reaction in a catalytic membrane reactor, the methane conversion, C_{2+} selectivity, C_{2+} yield and oxygen permeation flux are defined as [13]:

CH_4 conversion,

$$X_{CH_4} = \frac{F_{CH_{4,in}} - F_{CH_{4,out}}}{F_{CH_{4,in}}} \times 100\% \quad (1)$$

C_{2+} selectivity,

$$S_{C_{2+}} = \frac{2 \times (F_{C_2H_4} + F_{C_2H_6}) + 3 \times F_{C_3H_6}}{F_{CO} + F_{CO_2} + 2 \times (F_{C_2H_4} + F_{C_2H_6}) + 3 \times F_{C_3H_6}} \times 100\% \quad (2)$$

C_{2+} yield,

$$Y_{C_{2+}} = X_{CH_4} \times S_{C_{2+}} \quad (3)$$

O_2 flux,

$$J_{O_2} = \frac{F_{CO} + 2F_{CO_2} + F_{H_2O} + 2F_{O_2(unreacted)}}{2A_{surf}} \quad (4)$$

F_i is the flow rate of the species in mol/s and A_{surf} is the membrane surface area in cm^2. The concentration of gases in the feed and product was obtained from the on-line GC analysis. The conversion, selectivity and yield of the individual species were calculated from the compositions. The performance of catalytic membrane reactor is influenced by many operating parameters such as temperature, gas hourly space velocity, methane to oxygen ratio and dilution ratio.

In a typical experimental run, the furnace was heated to the reaction temperature 700–900 °C. A flow of the mixture of O_2 and N_2 gases were passed into the shell side at the rate of 150 cm^3/min for certain time, allowing the oxygen gas to permeate through the membrane to the tube side before the OCM reaction. Oxygen flow rate was maintained constant and the methane flow rate was manipulated to providing CH_4/O_2 ratio from 0.5 to 3 during the experimental tests. Once the furnace temperature reached constant value, the reaction was started by introducing methane from the tube side. The steady state was reached after about an hour and the product was sent to an online gas chromatograph for analysis. Each analysis took about 25 min and the total flow rate of the cooled product gases was measured using bubble flow meter. The reaction products were analyzed using on-line gas chromatograph HP 6890 equipped with FID, using a Poropak Q column for the separation of CH_4, C_2H_4, C_2H_6 and C_3H_8, and TCD, using a 0.5 nm molecular sieve column for the separation of H_2, O_2, CO_2, N_2 and CO.

2.5. Characterization

2.5.1. Scanning electron microscopy (SEM)

SEM was used to measure the film thickness and to study the membrane surface morphology of the inner surface, outer surface and cross-sectional view of the membrane. A scanning electron microscope (Zeiss Supra 35VP) equipped with W-Tungsten filament (Lanthanum-Hexabonde Field Emission) was used at 10–15 kV speed voltage, 155 eV resolution and orientation of 35° with Mn Kα as the energy source. The membrane tube was first cracked into small pieces, glued to the sample plate by double-sided tape and coated with a thin layer (~20 nm thick) of gold for electron reflection using Polaron Division Bio-RAD SEM sputter coater. The plate with the sample was then placed in the electron microscope for the analysis under magnification (300–50,000×).

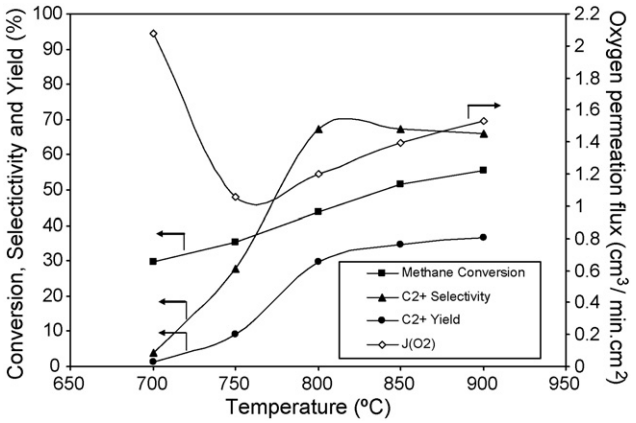

Fig. 3. Temperature profile of OCM reaction in catalytic membrane reactor with CH_4/O_2 ratio = 3, air flow rate = 150 cm^3/min and mixture of 48.6% CH_4 and 51.4% He = 194.5 cm^3/min.

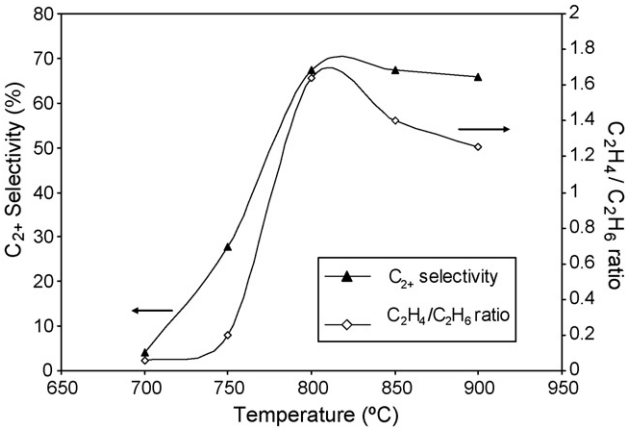

Fig. 4. Temperature dependence of C_2H_4/C_2H_6 ratio in OCM reaction with CH_4/O_2 ratio = 3, air flow rate = 150 cm^3/min and mixture of 48.6% CH_4 and 51.4% He = 194.5 cm^3/min.

2.5.2. High resolution X-ray diffraction (HR-XRD)

The crystalline phases of the membrane thin film were analyzed using high-resolution X-ray diffractometer system (PANalytical X'Pert Pro MRD PW3040, Spectris plc) with the integrated software, X'Pert HighScore. The HR-XRD system accepts the sample of either powder or thin film coated materials in the original form. The analysis of the MIEC membrane thin film coated on the alumina support with lanthanum oxides and the catalytic thin film on the support using XRD could provide important information. Any interaction between the interfacial layers could be detected by examining the crystalline phases of the XRD pattern. The source of the diffractometer is Cu Kα and Kβ monochromatic radiation with wavelength of 0.1541874 nm and 0.139225 nm, respectively. It is operated at 40 kV and 30 mA with the scattering angles at 2θ values of 10–80° with a step of 1.2°/min at room temperature.

3. Results and discussion

3.1. Oxidative coupling of methane

3.1.1. Effect of temperature

The effect of temperature to the performance of catalytic membrane reactor in OCM reaction is presented in Fig. 3. The air (mixture of oxygen and nitrogen) flow rate was maintained at 150 cm^3/min and CH_4/O_2 flow rate ratio at 3. The methane conversion, C_{2+} selectivity and yield of C_{2+} were increased with the increase of temperature (700–900°C). However, the C_{2+} selectivity was quite poor in the region of low temperature, indicates that lower temperature is less conducive to the C_{2+} formation due to the low catalytic activity. In contrast, the oxygen permeation flux obtained was 2.1 $cm^3/min\,cm^2$, which was remarkably higher at low temperature (700 °C), although the C_{2+} formation was very poor. The high concentration of oxygen at the reaction side was attributed to the faster oxygen permeation rate than the reactions of lattice oxygen with absorbed methane species and ethane species. It was observed that the oxygen permeation flux dropped at the temperature 750 °C but started to ascend moderately with the increment of temperature. The rise of oxygen permeation flux after 750 °C was mainly influenced by the active OCM reaction as the methane conversion and C_{2+} selectivity increased with respect to temperature, leading to the greater oxygen partial pressure gradient across the membrane. The highest C_{2+} selectivity of 67.5% was obtained at around 800–825 °C and started to decline after 900 °C.

The ethylene to ethane ratio in the catalytic membrane reactor was increased with the reaction temperature. Fig. 4 shows the influence of temperature over the C_{2+} selectivity and the C_2H_4/C_2H_6 ratio. It was found that the high temperature favored the formation of ethylene from ethane or the ethyl radicals, but it was limited to temperature of around 800 °C in the catalytic membrane reactor. The C_2H_4/C_2H_6 ratio started to descend when the temperature was increased beyond 800 °C because the tendency of ethane or ethyl radicals to react with oxygen for the formation of carbon oxides at the higher temperature.

The oxygen permeation flux under the OCM reaction conditions was compared with the one under pure helium condition without reaction (Fig. 5). In both situations air flow rate of 150 cm^3/min was fed to the shell side and helium (100 cm^3/min) at the tube side. When pure helium was passed in the tube side, the increment of oxygen permeation flux was quite insignificant, which was around 0.4–0.6 $cm^3/min\,cm^2$ at temperature range of 700–900 °C. Whereas, the introduction of methane during the OCM reaction greatly affected the oxygen flux, in such a way that most of the lattice oxygen that migrated from the oxygen-rich surface to the reaction surface and activated the methane. The oxygen flux under OCM condition was almost 3 times greater than the pure helium condition. Furthermore, the increment of the oxygen permeation flux was also remarkably higher. The performance of the oxygen permeation flux was different when there was OCM reaction at the permeate side.

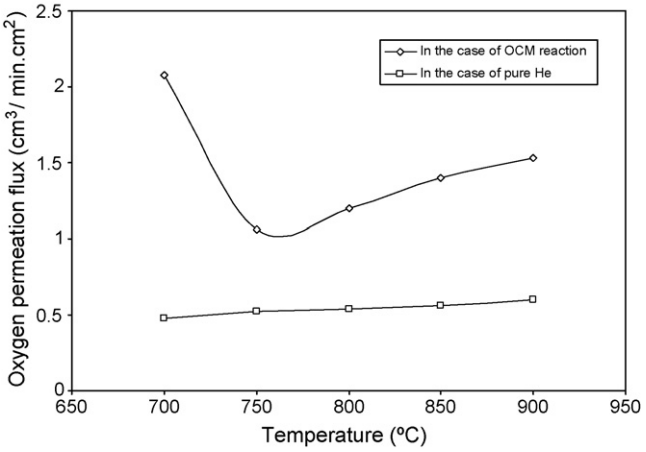

Fig. 5. Temperature dependence of oxygen permeation flux with or without reaction with air flow rate = 150 cm^3/min, CH_4/O_2 ratio = 3 and mixture of 48.6% CH_4 and 51.4% He = 194.5 cm^3/min.

Table 1
Effect of sweep gas flow rate to the performance of OCM reaction at $T = 850\,^{\circ}C$ and $CH_4/O_2 = 3$.

He flow rate (cm^3/min)	Methane conversion (%)	C_{2+} selectivity (%)	C_{2+} yield (%)	C_2H_4/C_2H_6 ratio	J_{O_2} with reaction (cm^3/min cm^2)	J_{O_2} with pure He (cm^3/min cm^2)
35	32.9 ± 1.4	2.5 ± 0.1	0.8 ± 0.2	1.0	2.2	0.2
100	51.6 ± 2.5	67.4 ± 3.4	34.7 ± 1.8	1.4	1.4	0.6

Fig. 6 shows the oxygen concentration of the total gas mixture at the tube side of the catalytic membrane reactor. The oxygen concentration without the introduction of OCM reaction was around 27–30% of the total gas mixture, without considering the helium content in the tube side. As the OCM reaction occurred, the oxygen concentration was 5.5–11% less than the former case albeit the oxygen permeation flux was higher as shown in Fig. 5.

3.1.2. Effect of methane to oxygen ratio

The effect of CH_4/O_2 ratio in the range of 0.5–3 over the OCM reaction is presented in Fig. 7. Methane conversion, C_{2+} selectivity and C_{2+} yield increased with the increase of CH_4/O_2 ratio. The oxygen permeation flux was observed inconsistent with the OCM results, in which the flux reduced with the increase of methane concentration in the tube side. The highest oxygen permeation flux was at 2.6 cm^3/min cm^2 and CH_4/O_2 ratio of 0.5, although the OCM activity was the lowest at this value. This was due to the recombination of lattice oxygen to gaseous oxygen predominantly occurred on the membrane surface exposed to OCM reaction. However, one could observe that the high oxygen flux reduced in a sliding pattern at the smaller CH_4/O_2 ratio but almost maintained at 1.5 cm^3/min cm^2 when the CH_4/O_2 ratio was within the range 2–3.

Low concentration of methane in the OCM reaction contributed little in the OCM activity, which was in agreement with the results reported in literature [13]. The greater degree of oxygen concentration at lower methane concentration shows that there is insufficient methane surface coverage on the membrane side exposed to reaction, allowing the recombination of lattice oxygen into gaseous oxygen [11]. The oxygen concentration in the tube side of the reactor reduced once the methane concentration was increased, as shown in Fig. 8. Therefore, it could be established that introducing more oxygen or the air flow rate would be meaningless because methane concentration is the one in controlling the performance of OCM reaction in the membrane reactor.

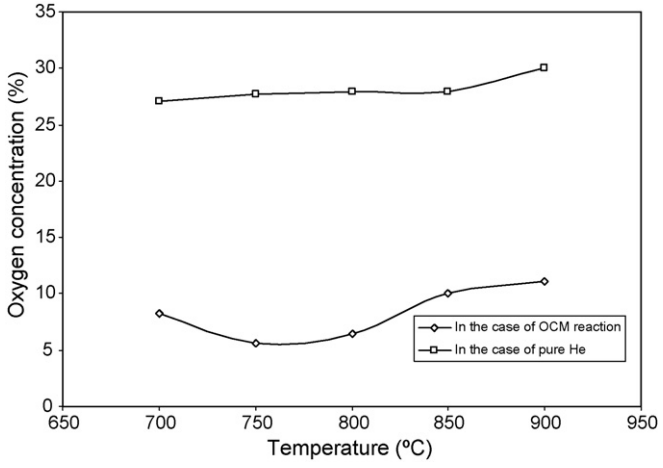

Fig. 6. Temperature dependence of oxygen concentration at the tube side with or without reaction with air flow rate = 150 cm^3/min, CH_4/O_2 ratio = 3 and mixture of 48.6% CH_4 and 51.4% He = 194.5 cm^3/min.

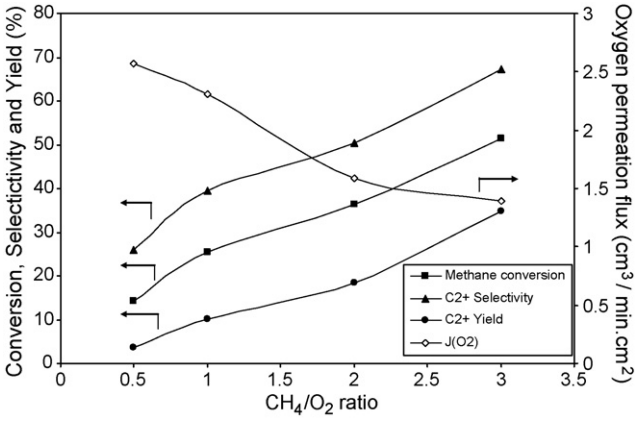

Fig. 7. Effect of CH_4/O_2 ratio over the performance of OCM process at temperature = 850 °C, air flow rate = 150 cm^3/min and He flow rate = 100 cm^3/min.

3.1.3. Effect of sweep gas flow rate

The effect of sweep gas flow rate to the performance of OCM reaction was studied at temperature 850 °C, air flow rate 150 cm^3/min and CH_4/O_2 ratio at 3 and presented in Table 1. It can be seen from the table that the sweep gas played an important role affecting the methane conversion, C_{2+} selectivity and C_{2+} yield. At helium gas flow rate 35 cm^3/min, 32.9% of methane conversion was obtained as compared to 51.6% methane conversion at higher sweep gas flow rate. A dramatic change of C_{2+} selectivity from 35 to 100 cm^3/min of helium flow rate signified that sweep gas flow rate had greater effect over the selectivity than the methane conversion. It was be due to more helium could sweep off the C_{2+} product from the reaction site and shortening the contact time between the intermediate products with the oxygen, thus resulting in higher C_{2+} selectivity by limiting the formation of carbon oxides. The oxygen permeation flux was higher in the presence of reaction, especially when the reaction rates were lower.

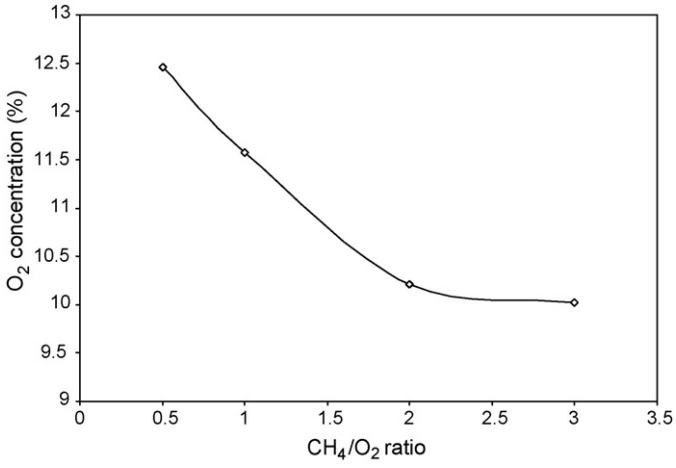

Fig. 8. Effect of CH_4/O_2 ratio over the oxygen concentration at the tube side at temperature = 850 °C, air flow rate = 150 cm^3/min and He flow rate = 100 cm^3/min.

Table 2
Comparison of CMR and PBCR at $T = 850\,^{\circ}C$ and CH_4/O_2 ratio = 3 with varying the dilution ratio.

Type of reactor	Helium flow rate = 100 cm^3/min			Helium flow rate = 35 cm^3/min		
	CH_4 conversion (%)	C_{2+} selectivity (%)	C_{2+} yield (%)	CH_4 conversion (%)	C_{2+} selectivity (%)	C_{2+} yield (%)
Packed bed catalytic reactor (PBCR)	49.3 ± 2.5	30.9 ± 1.5	15.2 ± 0.8	29.6 ± 1.5	46.1 ± 2.3	13.6 ± 0.7
Catalytic membrane reactor (CMR)	51.6 ± 2.6	67.4 ± 3.4	34.7 ± 1.7	32.9 ± 1.6	2.5 ± 0.1	0.8 ± 0.04

3.2. Comparison of OCM process in different reactor configurations

The performances of packed bed catalytic reactor (PBCR), CMR and packed bed catalytic membrane reactor (PBCMR) are compared for the purpose of investigating the most suitable design of reactor in the OCM process. The reactant feed mode that related to the reactor configurations is one of the important factors that affects C_{2+} selectivity, in which co-feed mode was used in PBCR, whereas PBCMR and CMR were both using separated-feed mode.

3.2.1. Comparison of catalytic membrane reactor and packed bed catalytic reactor

The comparison of a catalytic membrane reactor and packed bed catalytic reactor at temperature 850 °C, CH_4/O_2 ratio at 3 and varying dilution ratio is presented in Table 2. In CMR, helium was used as the diluents' and fed at 35 and 100 cm^3/min for low and high dilution, respectively. Both reactors gave different performances depending upon the operating conditions. The C_{2+} selectivity in CMR differed from 2.5% to 67.4% and influenced greatly by the diluents' flow rate (sweep gas) in the tube side. Whereas, PBCR performed conversely from the CMR, in which high dilution gave higher methane conversion but lower C_{2+} selectivity, and vice versa.

Compared to PBCR, the gaseous oxygen that was fed from the shell side of CMR has to undergo the adsorption of oxygen and charge transfer reaction on the membrane surface to the formation of lattice oxygen and electron hole, in which lattice oxygen has greater tendency to activate methane molecule to methyl radicals; whereas, the co-feed mode in PBCR implied the need of oxygen to be transformed to active species before activation of methane could take place. Therefore, the OCM reaction occurred at a higher rate in CMR than PBCR and higher dilution rate is believed to be more advantageous in providing higher C_{2+} selectivity in CMR.

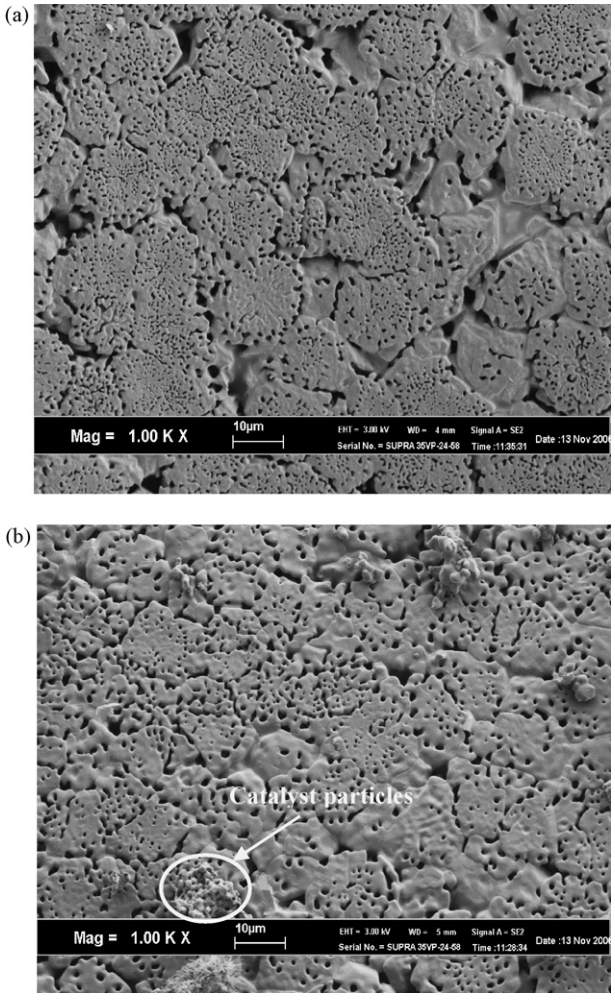

Fig. 9. SEM micrograph of surface morphology of the (a) fresh and (b) used Na-W-Mn/SiO_2 catalytic layer.

3.2.2. Comparison of packed bed catalytic membrane reactor and packed bed catalytic reactor

The PBCMR resembled the design of catalytic membrane reactor, except a 3 component catalyst was loaded in the membrane tube and tested under optimum condition (temperature = 850 °C, GHSV = 23,947 $cm^3/g\,h$, time of catalyst pretreatment = 2 h, dilution ratio = 0.2 and CH_4/O_2 ratio = 7) that obtained from process study of PBCR [21]. The performance of PBCR and PBCMR during the optimum condition was compared and presented in Table 3.

The overall results showed that PBCR has better performance than PBCMR with 43.1% methane conversion and 70.6% C_{2+} selectivity. The poor performance of PBCMR was most probably due to the bypass of the oxygen from the catalyst bed, resulting in the lower catalytic activity in the catalyst zone. Besides, the existence of catalyst bed in the membrane tube was believed to contribute pressure drop difference between the tube side and shell side, allowing the flow of mixture permeated from the tube side to the shell side. The activity test in PBCMR was carried out under optimum condition with and without sweep gas in the tube side. The presence of sweep gas significantly enhanced the C_{2+} selectivity from 20.8% to 55.5%, although the methane conversion did not vary much. However, it was observed that the optimum condition was only obtained from the process study using PBCR, which by no means in signifying these conditions would be the optimum conditions for PBCMR. The C_{2+} yield obtained from PBCMR was 20–25% lower than PBCR (30%), concerning that the C_{2+} selectivity obtained from PBCMR with helium was comparable to PBCR. C_{2+} selectivity could be enhanced by increasing the sweep gas flow rate in PBCMR but the gas bypassing problem must be solved in order to achieve higher methane conversion Thus, both the C_{2+} selectivity and methane conversion were equally important in performing high yield of C_{2+} products.

Table 3
Comparison PBCMR and PBCR at $T = 850\,^{\circ}C$, GHSV = 23,947 $cm^3/g\,h$, catalyst pretreatment period = 2 h, dilution ratio = 0.2 and CH_4/O_2 ratio = 7.

Type of reactor	CH_4 conversion (%)	C_{2+} selectivity (%)	C_{2+} yield (%)
PBCR	43.1 ± 2.2	70.6 ± 3.5	30.4 ± 1.5
PBCMR with sweep gas	12.9 ± 0.6	55.5 ± 2.8	7.1 ± 0.4
PBCMR without sweep gas	11.1 ± 0.6	20.8 ± 1.0	2.3 ± 0.1

Table 4
Comparison of CMR and PBCMR performances at $T = 850\,^{\circ}C$, $CH_4/O_2 = 3$, air flow rate = 150 cm^3/min and He flow rate = 100 cm^3/min.

Reactor type	Methane conversion (%)	C_{2+} selectivity (%)	C_{2+} yield (%)	J_{O_2} (cm^3/min cm^2)
Catalytic membrane reactor (CMR)	51.6 ± 2.6	67.4 ± 3.4	34.7 ± 1.7	1.4
Packed bed catalytic membrane reactor (PBCMR)	36.4 ± 1.8	39.6 ± 2.0	14.4 ± 0.7	1.2

3.2.3. Comparison of catalytic membrane reactor and packed bed catalytic membrane reactor

The performances of CMR and PBCMR were compared at temperature 850 °C, sweep gas flow rate 100 cm^3/min, air flow rate 150 cm^3/min and CH_4/O_2 ratio of 3 (Table 4). CMR showed its superiority over PBCMR with higher methane conversion and C_{2+} selectivity. The C_{2+} yield obtained from CMR was almost 2.5 times greater with 34.7%. Compared to PBCMR, the CMR has greater reaction site along the surface of the membrane tube inducing higher reaction rate, whereas the PBCMR was restricted to the area of the catalyst zone. The oxygen permeation fluxes in both reactor types did not differ much. These results might not the best results because the performances of these reactors might be better or worse depending upon the reaction conditions. Both the CMR and PBCMR still encountered some defects and problems in providing better results. The PBCMR might have better performance if the pressure drop of the catalyst bed could be minimized until a limit that the driving of products from tube side to shell side would not take place.

Catalytic membrane reactor performed the best results among three of the reactors with C_{2+} yield of 34.7%. However, the C_{2+} selectivity could be improved by well tuning the sweep gas flow rate and reactants concentration. Packed bed catalytic membrane reactor with the function as oxygen distributor was expected to have better performance than packed bed catalytic reactor, but it might due to the operating conditions that affecting the performance of PBCMR.

3.3. Characterization

3.3.1. SEM

The fresh and used catalytic layers coated on the lanthanum-modified γ-alumina surface are exhibited in Fig. 9(a) and (b), respectively. The catalytic layer was prepared by dip coating the colloidal form of Na-W-Mn/SiO_2 catalyst. The surface morphology of the catalytic layer was distributed with porous pattern, resulted from the evaporation of water molecules during the heating and calcination of the catalyst.

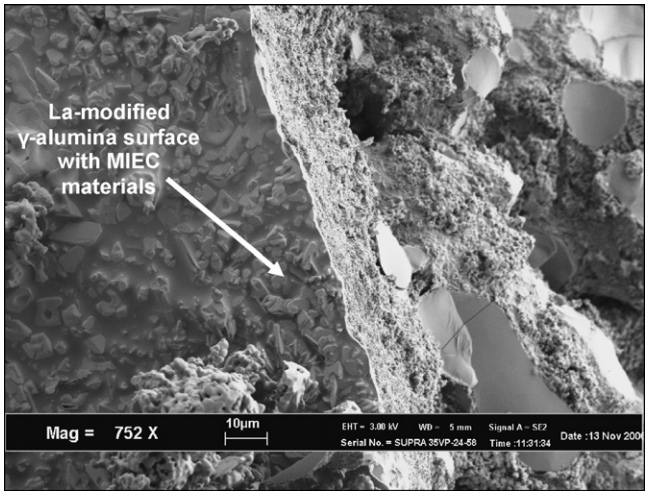

Fig. 10. SEM micrograph of surface morphology of the inner surface after reaction.

The used catalyst after the long-exposure to OCM reaction seemed to be sintered where some of the void enlargement was observed. Some catalyst particles (encircled part in Fig. 9(b)) appeared on the surface of the used catalytic layer, which came from the catalyst bed that was packed in the membrane tube during the activity test of packed bed catalytic membrane reactor. In order to investigate the surface morphology of the γ-alumina, the catalytic layer was removed and different shapes of crystals were found to be embedded in the layer (Fig. 10), implying that either the infiltration of catalyst from the inner surface or the MIEC materials from the outer surface (α-alumina) to the γ-alumina layer. It also shows the infiltration of MIEC materials from the outer surface to the γ-alumina layer, which filled the void between α-alumina particles.

3.3.2. HR-XRD

The XRD patterns of fresh and used membrane are shown in Figs. 11 and 12 respectively. The peaks of the components were found to overlap over each other and difficult to analyze the results. The elements that appeared for the relevant peaks were obtained from the library database of the PANalytical software. The perovskite $Ba_{0.5}Ce_{0.4}Gd_{0.1}Co_{0.8}Fe_{0.2}O_{3-\delta}$ phase was not found in the database because this mixed oxides material has a particular composition and hitherto is not reported in literature yet.

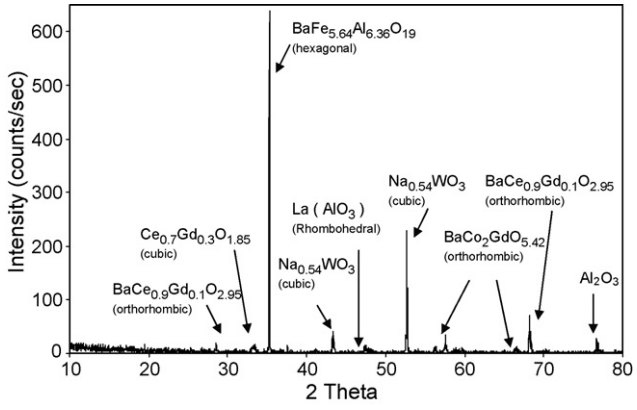

Fig. 11. XRD pattern of fresh $Ba_{0.5}Ce_{0.4}Gd_{0.1}Co_{0.8}Fe_{0.2}O_{3-\delta}$ membrane.

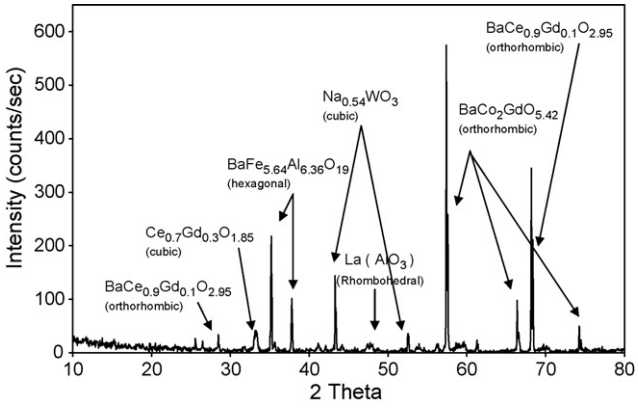

Fig. 12. XRD pattern of used $Ba_{0.5}Ce_{0.4}Gd_{0.1}Co_{0.8}Fe_{0.2}O_{3-\delta}$ membrane.

The existence of orthorhombic and cubic crystalline phases showed the distortion of perovskite phase to brownmillerite during the synthesis and heat treatment of the membrane. $BaFe_{5.64}Al_{6.36}O_{19}$ and Al_2O_3 were detected at 2θ value of 35° but the intensity of this peak decreased almost 3 times indicated that there were changes after the OCM reaction. Several peaks were found to increase their intensities after reaction especially peak of $BaCe_{0.9}Gd_{0.1}O_{2.95}$ and $BaCo_2GdO_{5.42}$, implying the migration of the cation species, especially from the infiltrated bulk to the oxygen-enriched surface. The catalyst components Na, W, and Mn also migrated to the reaction surface after reaction, resulting in the lower intensity of the related peaks. The estimated components appeared at 2θ value of 53° were sodium tungstate ($Na_{0.54}WO_3$) and manganese oxide (Mn_3O_4), both in cubic form. The XRD patterns (Figs. 11 and 12) suggest that the interaction of the elements to form different combinations of mixed oxides took place during the preparation of the membrane.

4. Conclusions

The chemical reaction influenced the oxygen permeation rate through the membrane. The oxygen permeation flux, however, needs to be controlled by regulating the other parameters such as temperature, methane to oxygen ratio, sweep gas flow rate and WHSV because the greater the oxygen flux does not guarantee in providing higher yield of C_{2+} product. Higher concentration of oxygen ion in the methane-enriched side will tend to recombine to gaseous oxygen and react with intermediates to form carbon oxides. A comparative performance study of packed bed catalytic reactor, catalytic membrane reactor and packed bed catalytic membrane reactor showed that the catalyst in packed bed catalytic reactor gave highest C_{2+} selectivity. Each reactor behaved differently depending upon the operating conditions. The catalytic membrane reactor gave the highest yield of C_{2+} as 34.7% with methane conversion of 51.6% and C_{2+} selectivity of 67.4%. The packed bed catalytic membrane reactor did not perform well compared to packed bed catalytic reactor and catalytic membrane reactor due to the leakage of gas.

SEM and XRD analyses show that the migration of the cation species from the infiltrated bulk of the MIEC material to the oxygen-enriched surface took place during the OCM reaction. The surface morphology of the MIEC membrane was found to form clusters of crystals after the OCM reaction. The cation species migrated through the bulk membrane to the oxygen-enriched surface in order to balance the local electrical of the membrane during the oxygen permeation and OCM reaction on both sides of the membrane. The distortion of perovskite to brownmillerite structures of the MIEC materials was taken place during the heat treatment process as detected by XRD.

Acknowledgements

The authors would like to acknowledge the Universiti Sains Malaysia, Penang, Malaysia for financially supporting this project (FPP 2005/030) under University Short-Term Grant and Research University (RU) grant. Special thanks to National Science Fellowship as well in sponsoring the researcher (Chua Yen Thien).

References

[1] J. Coronas, M. Menendez, J. Santamaria, Chem. Eng. Sci. 49 (1994) 2015–2025.
[2] J. Coronas, M. Menendez, J. Santamaria, Chem. Eng. Sci. 49 (1994) 4749–4757.
[3] D. Lafarga, J. Santamaria, M. Menendez, Chem. Eng. Sci. 49 (1994) 2005–2013.
[4] Y.K. Kao, L. Lei, Y.S. Lin, Catal. Today 82 (2003) 255–273.
[5] Y. Lu, A.G. Dixon, W.R. Moser, Y.H. Ma, Chem. Eng. Sci. 55 (2000) 4901–4912.
[6] N. Che May, A.R. Mohamed, S. Bhatia, The Regional Symposium of Chemical Engineers (RSCE), Kuala Lumpur, 28–30th October, 2002.
[7] Y. Lu, A.G. Dixon, W.R. Moser, Y.H. Ma, U. Balachandran, J. Membr. Sci. 170 (2000) 27–34.
[8] Z. Shao, H. Dong, G. Xiong, Y. Cong, W. Yang, J. Membr. Sci. 183 (2001) 181–192.
[9] X.M. Guo, K. Hidajat, C.B. Ching, Ind. Eng. Chem. Res. 36 (1997) 3576–3582.
[10] J. Langguth, R. Dittmeyer, H. Hofmann, G. Tomandl, Appl. Catal. A: Gen. 158 (1997) 287–305.
[11] S.J. Xu, W.J. Thomson, AIChE 43 (1997) 2731–2740.
[12] F.T. Akin, Y.S. Lin, J. Membr. Sci. 231 (2004) 133–146.
[13] W. Yang, H. Wang, Y. Cong, Catal. Today 104 (2005) 160–167.
[14] T. Nozaki, O. Yamazaki, K. Omata, K. Fujimoto, Chem. Eng. Sci. 47 (1992) 2945–2950.
[15] Y. Zeng, Y.S. Lin, J. Catal. 193 (2000) 58–64.
[16] S. Haag, A.C. vanVeen, C. Mirodatos, Catal. Today 127 (2007) 157–164.
[17] A.L. Shaula, A.P. Viskup, V.V. Kharton, D.I. Logvinovich, E.N. Naumovich, J.R. Frade, F.M.B. Marques, Mater. Res. Bull. 38 (2003) 353–362.
[18] L. Yang, X. Gu, L. Tan, L. Zhang, C. Wang, N. Xu, Sep. Puri. Technol. 32 (2003) 301–306.
[19] Z. Shao, W. Yang, Y. Cong, H. Dong, J. Tong, G. Xiong, J. Membr. Sci. 172 (2000) 177–188.
[20] J. Wang, L. Chou, B. Zhang, H. Song, J. Zhao, J. Yang, S. Li, J. Mol. Catal. A: Chem. 245 (2005) 272–277.
[21] Y.T. Chua, A.R. Mohamed, S. Bhatia, J. Chem. Technol. Biotechnol. 82 (2006) 81–91.